Scanning Microscopy Vol. 11, 1997 (Pages 417-425) 0891-7035/97$5.00+.25
Scanning Microscopy International, Chicago (AMF O'Hare), IL 60666 USA

DIFFERENTIAL MICROSCOPY IN OFF-AXIS TRANSMISSION ELECTRON MICROSCOPE HOLOGRAPHY

T. Tanji[1]* and T. Hirayama[2]

[1]Center for Integrated Research in Science and Engineering, Nagoya University, Nagoya, Japan
[2]Japan Fine Ceramics Center, Atsuta, Nagoya, Japan

Abstract

Differential microscopy is realized by conventional off-axis electron holography with an electron biprism behind the specimen. Two phase images reconstructed from two holograms obtained with slightly different potentials of the electron biprism are utilized to make a one-dimensional differential image. Polystyrene latex particles which are charged by electron irradiation and a barium ferrite particle which has a single magnetic domain were used to demonstrate that the differential image is independent of the distortion of the reference wave.

Key Words: Electron holography, differential interferometry, differential phase contrast, long range field.

*Address for correspondence:
T. Tanji
Center for Integrated Research in Science and Engineering (CIRSE)
Nagoya University
Chikusa, Nagoya 464-8603, Japan
Telephone number: +81-52-789-4436
FAX number: +81-52-789-3155
E-mail: tanji@cirse.nagoya-u.ac.jp

Introduction

A transmission electron microscope equipped with a field-emission electron gun (FE-TEM) makes it possible to construct an electron holographic interferometer using an electron biprism [18]. Off-axis electron holography has been successfully used in the observation of phase objects such as magnetic fields [4, 17] and electrostatic potentials [2, 10]. Off-axis electron holography can reveal the distribution of magnetic flux density and inner potentials of substances if such a magnetic or electric field is localized into a small region. In off-axis holography, a well defined reference wave is indispensable for evaluation of the interference fringes. In many cases, however, the magnetic or electric field extends beyond the lateral coherence length of the electrons, which means that only the phase difference between an object wave and the reference wave is obtained. As a result, the information extracted from the hologram with the distorted reference wave does not accurately express the fields or the potentials of the object. Moreover, for the observation of magnetic substances, a distortion-free or plane reference wave restricts the observation area to the region near the edge of the specimen. The magnetic lines of force near the specimen edge are liable to close inside to suppress the leakage of flux into a vacuum; therefore, the magnetic structures inside are often of interest to us.

One of the ways to surmount this problem of the distorted reference wave has been shown by Matteucci *et al*. [10]. Their analysis using a computer simulation can reveal an accurate field for some simple cases. Differential interferometry [13], a typical example of shearing interferometry, is another useful method for observing phase objects when a plane reference wave cannot be obtained.

With regard to electron holographic interferometry, some configurations have been reported for differential interferometry. They illuminate the specimen with two coherent electron beams inclined toward each other by using a beam splitter placed in front of the specimen. Leuthner *et al*. [8] and Takahashi *et al*. [14] installed an electron biprism in the illumination system of a scanning transmission electron microscope (STEM) equipped with a detection system that has a reference grating. The reported resolution

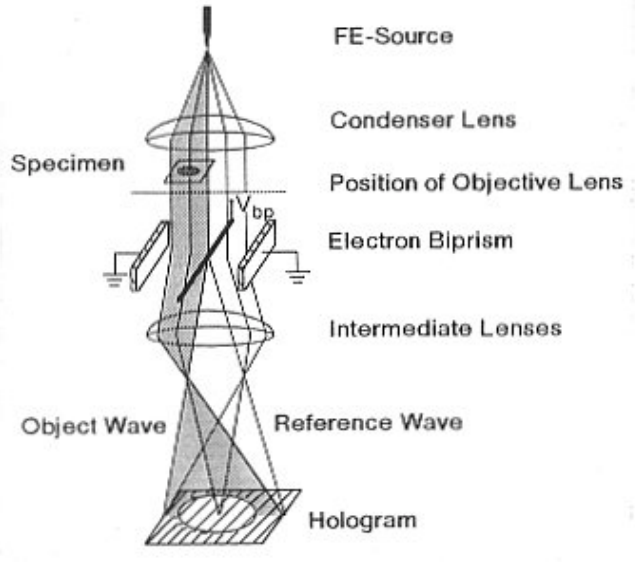

Figure 1. Schematic electron-optical system for electron holographic interferometry. V_{bp} = potential of the biprism.

of this scanning-type interferometer is not very high so far (> 5 nm). A projection-type differential interferometer has been reported by Mankos *et al*. [9]. They utilized the same STEM configuration to make interference fringes in a shadow image and showed magnetic domains in a cobalt film. Their interferometer, however, requires intrinsically larger defocusing of the object for a larger interference region. Kruit and Buist [5] used a crystalline beam splitter inserted into a TEM instrument equipped with an ordinary thermionic electron gun. Their technique requires that the crystalline beam splitter has a large uniform area of orientation and thickness and that it is inflexible of changing the fringe spacing. They are both obstacles in practical applications. These disadvantages of the last two types of interferometers may be overcome by installing the electron biprism in the illumination system of the FE-TEM instrument [6, 11]. On the other hand, in conventional electron off-axis holography [18], using the FE-TEM instrument which has an electron biprism behind the specimen (off-axis TEM holography), the interference region is limited by only the lateral coherent length of the electron waves. A resolution higher than STEM holography is easy achievable [12, 15] with off-axis TEM holography, which has improved the precision of its phase measurement [7], but sufficiently small shearing of the object wave has been impossible. If two holograms, which have a slight difference in the sheared regions of their object wave by the reference wave, are recorded, then the interference of the two object waves reconstructed from these holograms offers shearing interferometry. When the amount of the shearing is sufficiently small, this interference pattern corresponds to the differential of the phase of the object wave. Today, we can reconstruct the phase numerically and can directly obtain its differentiation. In this paper, preliminary results of differential microscopy by off-axis TEM holography are reported for the electrostatic potential around charged polystyrene latex particles and a barium ferrite particle which has a single magnetic domain.

Principle

The phase increment of an electron beam transmitted through an electromagnetic potential ($\boldsymbol{A}$,V) is derived from the Schrödinger equation with the Wentzel-Kramers-Brillouin (WKB) approximation [1] as,

$$\phi = \frac{2\pi}{\hbar}\int_{L}(m\mathrm{v} \qquad (1)$$

where $eV = (1/2)m\,|\boldsymbol{v}|^2$, L is an electron trajectory, $\hbar$ is Planck's constant, and m, e and $\boldsymbol{v}$ are the mass, charge and velocity of the electron, respectively. When an additional electrostatic potential Vs, which is owing to an object, is small enough, the phase shift introduced by the first term of Equation (1) shows a difference of potentials projected along the two trajectories as

$$\phi = \frac{\pi}{\lambda Va}\int_{L_{12}} Vs\,dl\,, \qquad (2)$$

where Va and λ are the accelerating voltage and the electron wavelength, and integration is carried out along a closed path L_{12} connecting two electron trajectories. For a magnetostatic potential, the second term of Equation (1), ϕ directly corresponds to the magnetic flux passing through the surface S_{12} enclosed by the two trajectories as

$$\varphi = \frac{2\pi e}{\hbar}\int_{S_{12}} B_n\,ds \qquad (3)$$

where $\boldsymbol{B}_n$ is the component of the magnetic flux density normal to the surface S_{12}. Consequently, a one-dimensional differential image of the electron phase shows a component of the projected electric field $\boldsymbol{E}$ parallel to the differential direction and a perpendicular component of the projected magnetic flux density $\boldsymbol{B}$ [3, 19].

Electron holograms are generated by the interference of a modulated object wave and a plane reference wave as shown in Figure 1. If the specimen includes a long range field which extends into the reference wave, the phase reconstructed from the hologram is no longer the true phase distribution of the object wave. Instead, it reveals the phase difference between the object and the reference waves as illustrated in Figure 2, where long range field originating at the center of the object strongly modulates the

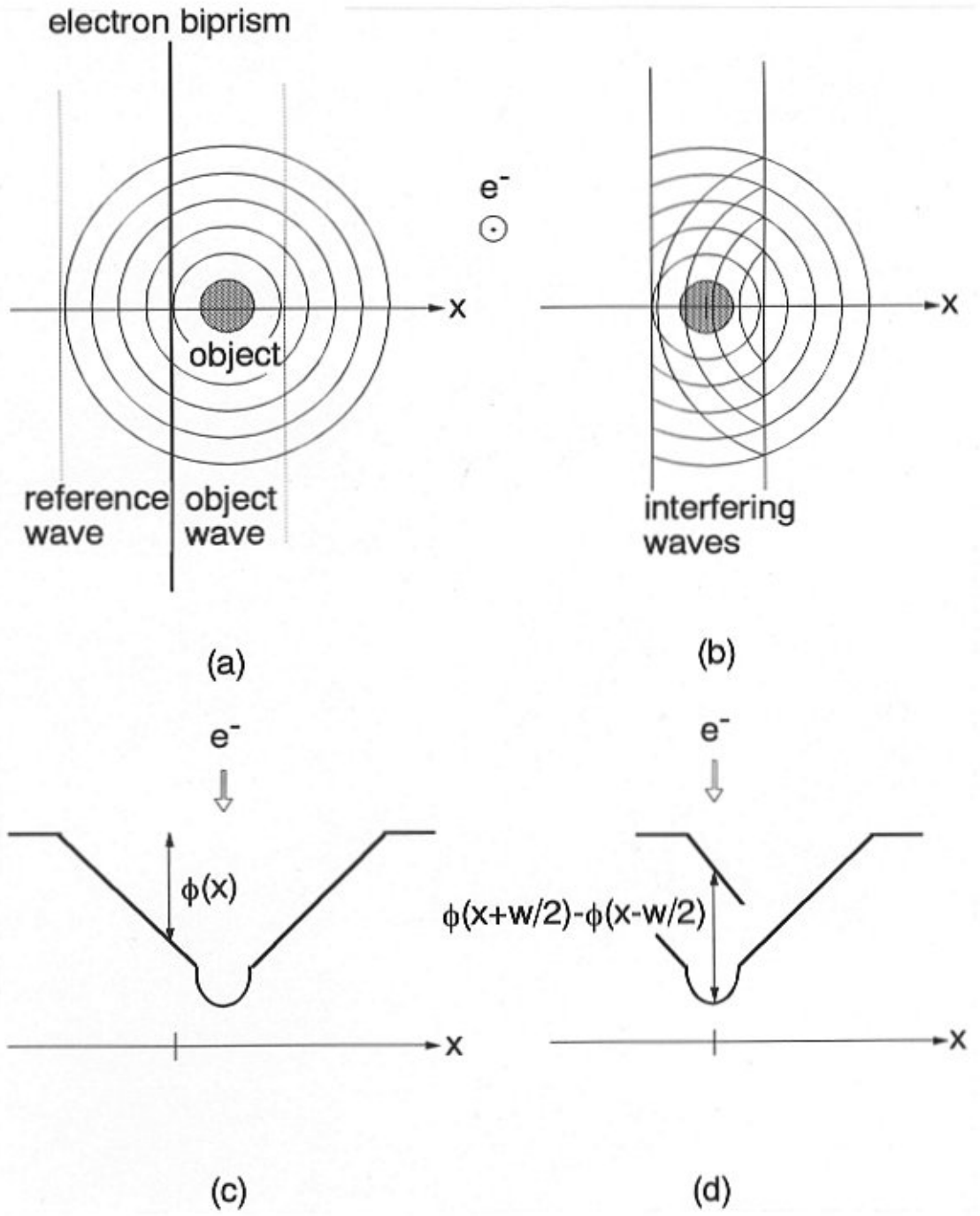

Figure 2. Equi-phase lines of an electron wave coming through a long range field (**a**) are overlapped by an electron biprism (**b**). It is obvious in cross sectional views that the phase reconstructed from the hologram is not the true phase distribution (**c**) but the difference between an object wave and a modulated reference wave (**d**). $\phi(x)$ = phase distribution; w = interference width.

referencewave and overlaps with the object in the hologram. In such a case, differential interferometry might be a powerful tool for accurately measuring the object phase.

The shearing of the interference region essential for the differential interferometry is achieved by changing the potential applied to the electron biprism, as illustrated in

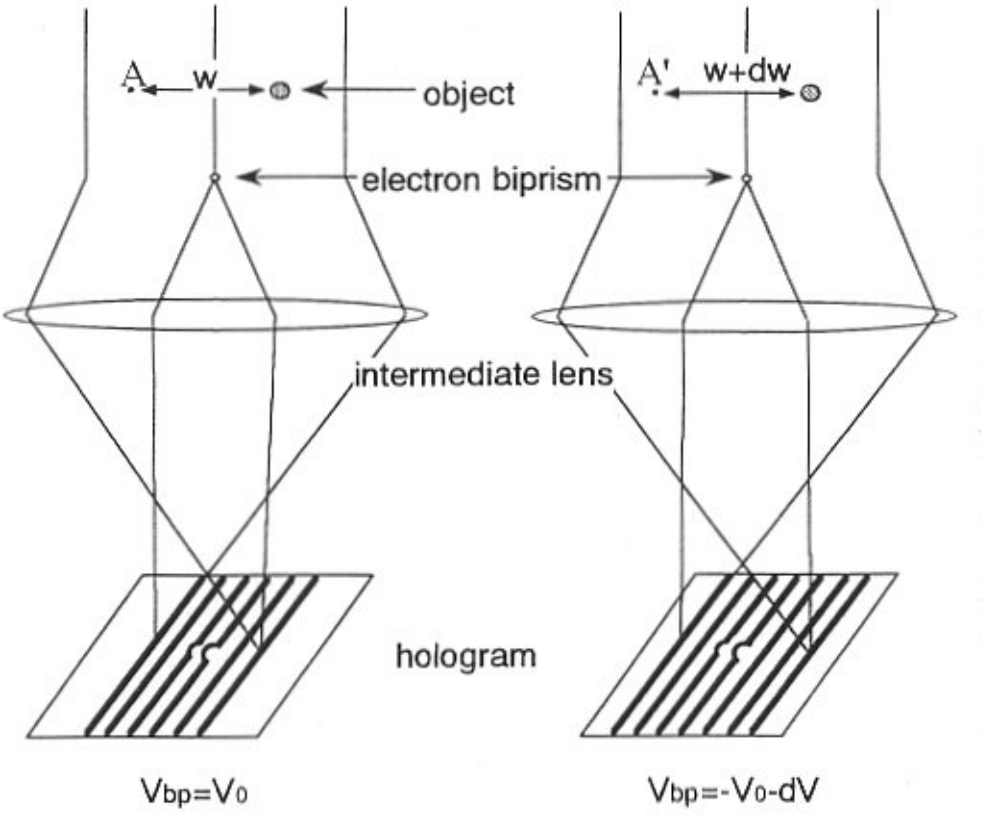

Figure 3. Reference point overlapped with an object is sheared from A to A' by increasing the potential applied to an electron biprism. V_{bp} = potential of the biprism; V_o = initial potential; w = initial interference width; dV = additi-onal potential; dw = expansion of the width.

Figure 3. Let the phase distribution of the electron after coming through the objective plane, $\phi(x)$, which extends over the reference region, and an object wave, $\psi(x) = \exp\{-i\phi(x)\}$, be overlapped to make a hologram with a reference wave, $\psi(x-w) = \exp\{-i\phi(x-w)\}$, at the potential of the biprism, $V_{bp} = V_0$. The amount of w is almost equal to the interference width. Assuming the magnification to be unity, and the coordinates of x to be common in the object and the hologram plane, the intensity of the hologram is expressed as

$$I(x) = \left| \psi(x+w/2)+\psi(x-w/2) \right|^2 \qquad (4)$$

and the phase image reconstructed from this hologram is [19]

$$\varphi_1(x) = \phi(x+w/2)-\phi(x-w/2). \qquad (5)$$

When V_{bp} changes to V_0+dV, the point overlapping with the object is sheared by dw from point A to A', and the second phase image,

$$\varphi_2(x) = \phi(x+w/2+dw/2)-\phi(x-w/2-dw/2) \qquad (6)$$

is reconstructed. Subtraction of these two images gives a differential of the original phase. Although both the object wave and the reference wave then shift against the observation coordinates, if we fix the position of the reference wave in the subtraction, we obtain the differential of the object wave as

$$\delta\phi(x) = \{\varphi_2(x-w/2+dw/2)-\varphi_1(x-w/2)\}/dw = \{\phi(x+dw)-\phi(x)\}/dw \qquad (7)$$

Fixing the position of the object, on the other hand, we have that of the reference wave $\delta\phi(x-w)$. This procedure can be realized by digital recording and processing systems.

When the phase shift of the object wave or the reference wave is large, determination of the carrier frequency is very difficult. In the Fourier transform reconstruction method, therefore, it is usual to refer to blank holograms recorded in a unperturbed vacuum area at each condition of the biprism.

Sometimes we may be able to reconstruct the original phase $\phi(x)$, which is free from the effect of the reference wave, by integrating $\delta\phi(x)$ along x-direction as,

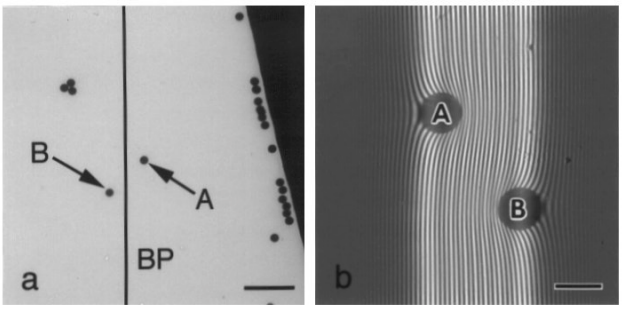

Figure 4. Low magnification transmission electron micrograph of polystyrene latex particles (ϕ = 1.0 μm) (**a**). Two spheres indicated with arrowheads (A and B) were recorded in an electron hologram (**b**) from both sides of an electron biprism (BP). Bars = 5 μm (in a) and 1 μm (in b).

$$\phi(x) = \int_{x_0}^{x} \delta\phi(x)\, dx + C\,, \qquad (8)$$

where x_0 is the edge of the interference region, and constant C shows the phase at the point x_0. If the integrated phase is one-dimensional, the constant C can be taken arbitrarily. In the case of two-dimensional phase distribution, however, values of C at x_0 for every line have to be determined or be replaced with an equal value in order to reconstruct a meaningful distribution.

Experiment

A Hitachi HF-2000 FE-TEM (Hitachi Ltd., Tokyo, Japan) equipped with a Gatan 679 (Gatan, Pleasanton, CA) slow-scan CCD camera was used to make holograms, and the processing was performed on a personal computer. The objective lens and condenser lenses were turned off, and two intermediate and two projective lenses were excited maximally, resulting in a magnification of 2000 times on a fluorescent screen. The exposure time was controlled not by a magnetic deflector (the usual system of Hitachi's electron microscopes combined with the slow-scan CCD camera), but by a mechanical shutter. This is essential in electron holography, because source drift, which is due to the time delay of ferrite cores of the deflector coils, causes the initial phase of the electron to drift. Typical exposure time was 20 seconds and readout time from the CCD to a frame memory was 2 seconds per frame of 1000 x 1000 pixels.

Results and Discussion

Figures 4 and 5 show the results obtained with differential microscopy of polystyrene latex particles of 1 μm in diameter charged by electron irradiation [16]. The electron wave, including two charged particles which are indicated by arrowheads in a low magnification transmission electron micrograph in Figure 4a, was superimposed by an electron biprism (BP) with V_{bp} = -13 V to make a hologram, Figure 4b, in which electric fields around the latex spheres modulate the reference waves. A blank hologram was obtained in a sufficiently far vacuum area at the same biprism condition and was used in order to reconstruct a phase image, Figure 5a, from which another phase image, Figure 5b, reconstructed from a hologram recorded with V_{bp} = -13.5 V, was subtracted. The amount of shearing, *dw*, was about 0.1 μm. The subtraction was performed to keep the coordinates of particle A the same in both reconstructed waves so that the potential around particle B is differentiated along the lateral direction in Figure 5c. The variance of the differentiated phase along the edge of the differentiated area (vertical direction) in Figure 5c is below $\pi/20$. This value is not so large considering the sensitivity of this preliminary work, and we can integrate the differential image so that the potential distribution, free from the effect of the reference wave, is revealed, as shown in Figure 5d. The dark band in Figure 5d is due to the indeterminable area in the phase that corresponds to particle A. As easily understood from Figure 4a, the asymmetrical distribution of the potential around B means the interaction with particle A, namely, the potential at the side facing particle A has a larger gradient than that at the other side.

Figure 6 shows the one dimensional differentiation of a Ba-ferrite particle. The larger particle in the transmission electron micrograph in Figure 6a has a single magnetic domain, as is recognized from the hologram (Fig. 6b; V_{bp} = -16.0 V) and a simply reconstructed phase image (Fig. 6c). Another phase image recorded with a slightly higher biprism potential (V_{bp} = -15.6 V) was subtracted from Figure 6c, yielding a differential image Figure 6d. The differentiation was performed along the horizontal axis, therefore, Figure 6d shows the vertical component of magnetic flux $\boldsymbol{B}$ around the particle as described in the **Principle** section. The dark contrast around the particle in Figure 6b is due to the effect of the biprism. Some part of the scattered waves at the crystal edge or deflected waves by the magnetic field was shaded by the biprism. However, the phase distribution of the electron wave is not as serious as the intensity distribution. Of course, the lack of information causes inaccuracy of phase measurement, and detailed investigation of this inaccuracy remains.

The accuracy of the differentiation is determined by the amount of shearing, which is controllable by supplying potential within the detectable limit of phase difference. In practice, however, it has to be noticed to keep the direction of shearing perpendicular to the prism wire. The shearing direction was often not exactly perpendicular to the prism wire, apparently owing to the inhomogeneous biprism field

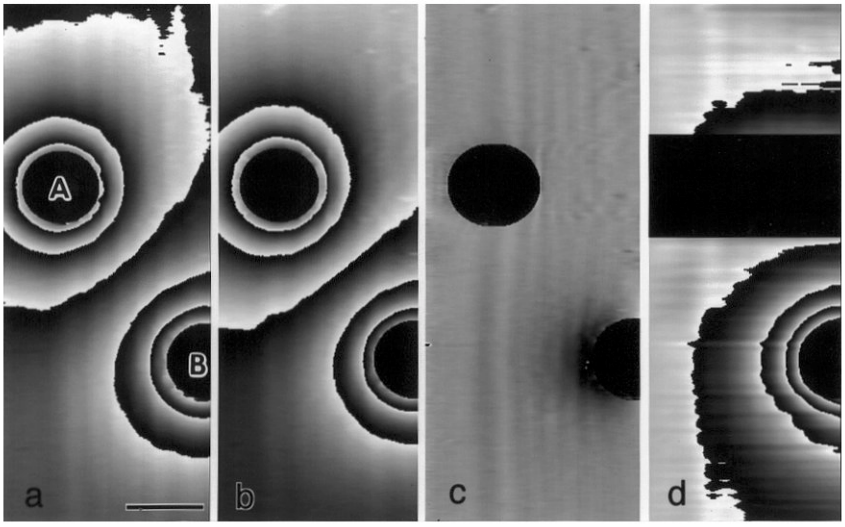

Figure 5. Differential interferometry of latex spheres [16]. (**a**) A phase image reconstructed from a hologram (fig. 4b) taken with the biprism potential V_{bp} = -13.0 V; (**b**) another phase image of V_{bp} = -13.5 V; (**c**) a one-dimensional differential image; and (**d**) integrated image showing a true phase distribution. Bar = 1 μm.

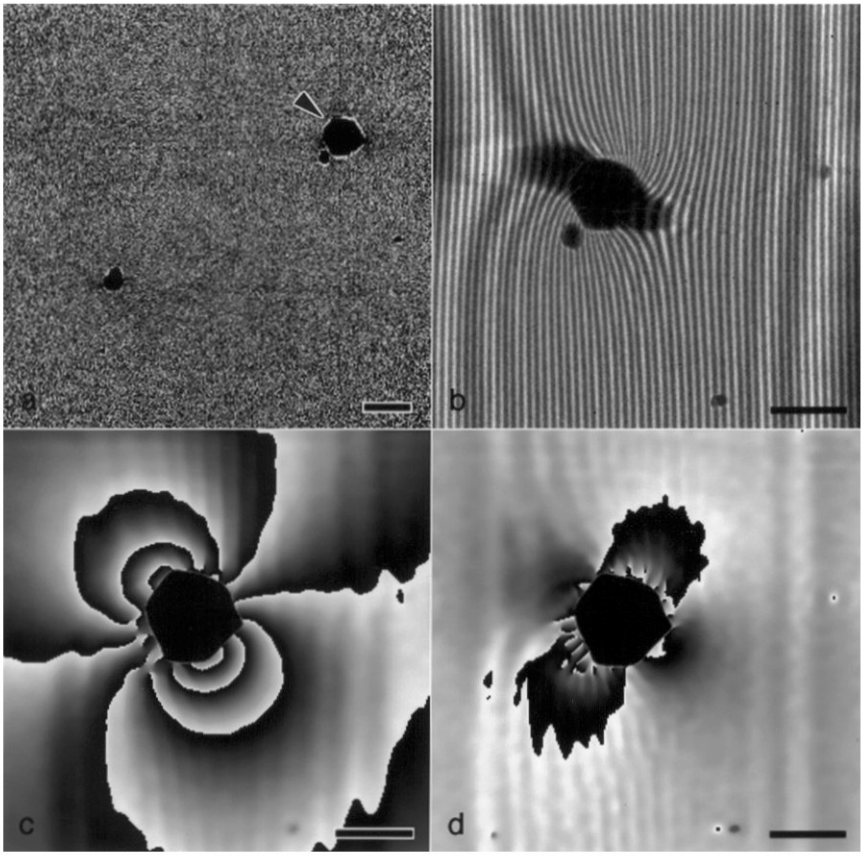

Figure 6. Differential interferometry of a magnetic field. (**a**) Low magnification trans-mission electron micrograph of Ba-ferrite particles. The particle indicated by an arrow-head was processed: (**b**) a hologram; (**c**) phase image reconstructed from (**b**) shows that it has a single magnetic domain; and (**d**) the differen-tial image denotes the vertical component of the magnetic field around the particle. Bars = 3 μm.

at the ends of the wire. This is especially important in two-dimensional differential interferometry.

Finally, we mention another kind of differential interferometry. If we realize a trapezoidal prism or a monoprism which does not deflect the reference wave but only the object wave as shown in Figure 7, we obtain a differential interferogram from one hologram. As the reference wave does not shift by changing the potential of the prism, we can use a double exposure technique, and the reconstructed intensity shows the differential of an object phase.

Conclusion

Electron differential interferometry was accom-

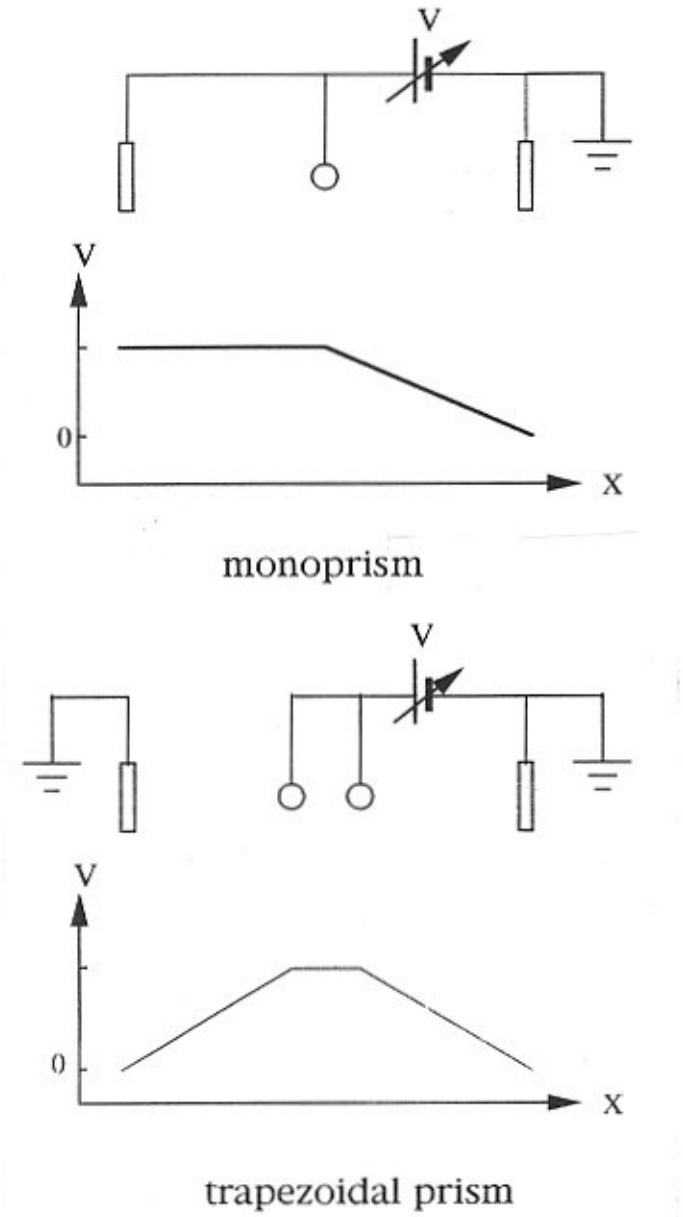

Figure 7. Monoprism and trapezoidal prism make it possible to reconstruct a differential interferogram from a double exposed hologram. x coordinates are perpendicular to the prism filaments; V = potential.

plished by conventional off-axis electron holography with an electron biprism behind a specimen. A serious effect of the distorted reference wave was eliminated clearly. The actual distribution of the electrostatic potential was reconstructed, and a component of the magnetic flux around a small particle was demonstrated. This technique, in combination with the high-precision phase measuring system already developed, will increase accuracy in measuring long range fields, such as electromagnetic fields.

Acknowledgments

Some parts of this work were done in Tonomura Electron Wavefront Project, ERATO, JRDC and in the Advanced Research Laboratory, Hitachi Ltd. The authors would like to thank Dr. Q. Ru of ERATO, JRDC for his computing support and Professor K. Goto and Mr. T. Sakurai of Tohoku University for preparing Ba-ferrite samples.

References

1. Ehrenberg W, Siday RE (1949) The refractive index in electron optics and the Principles of dynamics. Proc Phys Soc London B **62**: 8-21.

2. Frabboni S, Matteucci G, Pozzi G, Vanzi M (1985) Electron holographic observations of the electrostatic field associated with thin reverse-biased p-n junctions. Phys Rev Lett **55**: 2196-2199.

3. Hasegawa S, Kawasaki T, Endo J, Tonomura A, Honda Y, Futamoto M, Yoshida K, Kugiya F, Koizumi M (1989) Sensitivity-enhanced electron holography and its application to magnetic recording investigations. J Appl Phys **65**: 2000-2004.

4. Hirayama T, Ru Q, Tanji T, Tonomura A (1993) Observation of magnetic-domain states of barium ferrite particles by electron holography. Appl Phys Lett **63**: 418-420.

5. Kruit P, Buist AH (1994) Differential phase contrast in TEM. In: Proc of the 13th Int Cong Electron Microsc. Vol. 1. Jouffrey J, Colliex C (eds.). Les Editions de Physique Les Ulis, Paris, France. pp. 335-336.

6. Kruit P, Buist AH, McCartney MR, Scheinfein MR (1995) Differential phase contrast in TEM for magnetic micro structure observation. In: Proc. Microscopy and Microanalysis. Bailey GW, Ellisman MH, Hennigar RA, Zaluzec JJ (eds.). Jones and Begel Publishing, NY. pp. 606-607.

7. Lai G, Ru Q, Aoyama K, Tonomura A (1994) Electron-wave phase-shifting interferometry in transmission electron microscopy. J Appl Phys **76**: 39-45.

8. Leuthner T, Lichte H, Herrmann K-H (1988) STEM-holography using an electron biprism. In: Inst. Phys. Conf. Ser. No. 93. Vol. 1, (EUREM88). Institute of Physics, Bristol, U.K. pp. 177-178.

9. Mankos M, Scheinfein MR, Cowley JM (1994) Absolute magnetometry at nanometer transverse spatial resolution: Holography of thin cobalt films in a scanning transmission electron microscope. J Appl Phys **75**: 7418-7424.

10. Matteucci G, Missiroli GF, Muccini M, Pozzi G

(1992) Electron holography in the study of the electrostatic fields: The case of charged microtips. Ultramicroscopy **45**: 77-83.

11. McCartney MR, Kruit P, Buist AH, Scheinfein MR (1996) Differential phase contrast in TEM. Ultramicroscopy **65**: 179-186.

12. Orchowski A, Rau WD, Lichte H (1995) Electron holography surmounts resolution limit of electron microscopy. Phys Rev Lett **74**: 399-402.

13. Pluta M (1987) Holographic microscopy. In: Advanced in Electron and Optical Microscopy. Barer R, Cosslett VE (eds.). Academic Press, London. pp. 99-213.

14. Takahashi Y, Yajima Y, Ichikawa M, Kuroda K (1994) Observation of magnetic induction distribution by scanning interference electron microscopy. Jpn J Appl Phys **33**: L1352-L1354.

15. Tanji T, Ishizuka K (1994) Observation of crystal structures by using image restoration in electron holography. Microsc Soc Am Bull **24**: 494-500.

16. Tanji T, Ru Q, Tonomura A (1996) Differential microscopy by conventional electron off-axis holography. Appl Phys Lett **69**: 2623-2625.

17. Tonomura A (1989) Present and future of electron holography. J Electron Microsc **38**: S43-S50.

18. Tonomura A, Endo J, Matsuda T (1979) An application of electron holography to interference microscopy. Optik **53**: 143-146.

19. Urata K, Isizuka K, Tanji T, Tonomura A (1994) An application of digital filtering in electron holography at atomic resolution. J Electron Microsc **42**: 88-93.

Discussion with Reviewers

P. Kruit: According to Equation (7), you must first reconstruct the two images and then subtract the images. Is it not necessary to unwrap the phase before you do the subtraction? If not, how do you get rid of the large jump where one image is $2\pi+\delta\phi$ different from the other image?
Reviewer II: Is the reconstructed field still differentiated linearly?
Authors: In actuality, we performed the subtraction using two wave-functions, i.e.,

$$\exp\{i\delta\phi(x)dw\} = \exp\{i\varphi_2(x-w/2+dw/2)\}\exp\{-i\varphi_1(x-w/2)\},$$

then $\delta\phi(x)$ in Equation (7) was obtained. So, we did not need the phase unwrapping. This procedure is possible only if the amplitude of the object wave is uniform outside the particles.

P. Kruit: In general, in your experience, how large are the differential phases compared to the absolute phases that you measure in the images?
Authors: Although there is no meaning in comparing the differential phases to the absolute ones, the former is generally smaller than the latter, as shown in Figures 5 and 6.

P. Kruit: How do you interpret Figure 6d quantitatively?
Authors: For the contrast outside the particle, quantitative interpretation is not so easy, though it is possible qualitatively. That is, in the area where the reconstructed phase in Figure 6c changes rapidly in the lateral direction, the differential phase in Figure 6d shows darker or brighter contrast than other areas.

P. Kruit: Please describe the other kind of interferometry that you mention at the end of the **Results and Discussion** section? How can you get a differential interferogram by adding two holograms?
Authors: It is the same principle as a double exposure hologram. That is, we can record many wavefronts in one film (or other media) and reconstruct them simultaneously [13]. So the same interferometry as those consisting of two object electron waves [5, 6, 9, 11] is available.

Reviewer II: What is the effect of the charge in distance between spheres A and B when the biprism voltage is varied?
Authors: Varying of the biprism voltage causes no effect on the electrostatic potential of the object, including the leaking out potential. The effect of the charge means that the gradient of the potential is steeper between A and B than in other areas.

Reviewer II: The differentiation step is about 0.1 μm, so the resulting images should be probably averaged, as features below 0.1 μm may be artifacts.
Authors: We agree. With regard to the contrast outside the particle, the fine structure is due to the variation of the constant in Equation (8) (in Fig. 5d) and the effect of Fresnel fringes.

H. Lichte: Can you expand on the discussion of the effect that the overlapping direction is not perpendicular to the fringes.
Authors: Although this affects to the accuracy of results, it is a problem of experimental skill, and also, we can select data to keep the direction perpendicular to the fringes. Detailed discussions will also be necessary for more accurate experiments in future.

H. Lichte: Equation 1 says: "where $eV = (1/2)m\,|\,\boldsymbol{v}\,|^2$ ...."; why absolute modulus of $\boldsymbol{v}$?
Authors: Because $\boldsymbol{v}$ is a vector.

H. Lichte: If V is the potential of the object related to the accelerating voltage Va, then this relation is wrong. Instead it should read $e(Va+V) = (1/2)mv^2$.
Authors: This depends on the reference point of the potential. If we take the reference point at the vacuum just on the surface of a specimen, the V should be replaced by $V+Va$, but if we take the reference at the emitter, which is not so strange in general, potential V includes Va. The equation expresses a very general case. In order to avoid confusion, we replace the additional potential V in Equation (2) with Vs.

H. Lichte: In **Results and Discussions**, the authors state "However, the phase distribution of the electron wave is not as serious as the intensity distribution." Why is this true?
Authors: Actually, in the intensity distribution, the shadows by the biprism seem as if they were something real. On the other hand, the reconstructed phase does not show an abrupt change but continuous shift due to the magnetic field around such shadow areas in many cases. This is because only a part of the scattered wave is shaded by the prism, and the rest contributes to the imaging (interference fringes appear even in such shadows) and because the phase of electron wave tends to be continuous. But, as stated in the **Results and Discussion**, lack of information causes inaccuracy of phase measurement.

H. Lichte: Is resolution the point of this paper?
Authors: Yes, it is the only point at which using TEM holography may be superior to using STEM one in differential microscopy.